Langmuir

Article

pubs.acs.org/Langmuir

Temperature- and pH-Responsive Micelles with Collapsible Poly(*N*-isopropylacrylamide) Headgroups

Paul A. FitzGerald,[†] Sushen Gupta,[†] Kathleen Wood,[‡] Sébastien Perrier,[†] and Gregory G. Warr*[,†]

[†]The School of Chemistry, Building F11, The University of Sydney, Sydney, NSW 2006, Australia

[‡]Bragg Institute, ANSTO, Locked Bag 2001, Kirrawee DC, NSW 2232, Australia

Supporting Information

ABSTRACT: We have studied the micelle formation and phase behavior of a series of temperature- and pH-responsive surfactants prepared by controlled radical (RAFT) polymerization. These $C_{12}NIPAM_m$ surfactants consist of a dodecyl tail, a poly(*N*-isopropylacrylamide) (polyNIPAM) headgroup with average degrees of polymerization of between 7 and 96, and an ionizable carboxylate group. In the un-ionized state, these surfactants phase separate on warming toward a lower critical solution temperature (LCST), which decreases as the length of the NIPAM group is decreased. This is in agreement with the behavior of conventional nonionic poly(ethylene oxide)-based surfactants but is very different from that of polyNIPAM oligomer solutions. Small angle neutron scattering (SANS) shows that these surfactants self-assemble into micelles consisting of a nearly spherical hydrophobic core surrounded by a "hairy" polyNIPAM shell far below their LCST. Upon warming, the micelles undergo a sphere-to-rod transition induced by the collapse of the polyNIPAM shell, causing a reduction in the headgroup area. In the un-ionized state the demixing follows at the LCST, but a single charge on the free polymer end completely suppresses phase separation, allowing micelles to undergo a shape change but remain dissolved.

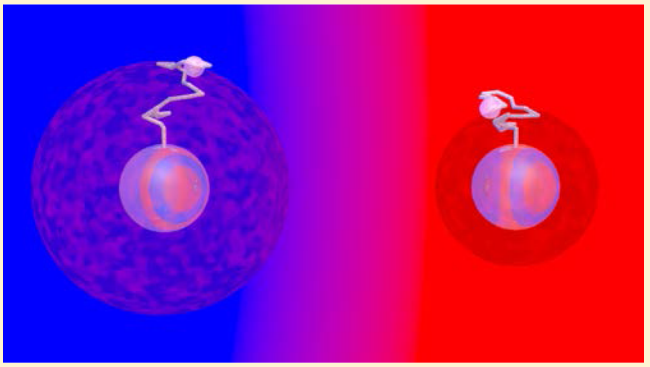

INTRODUCTION

Poly(*N*-isopropylacrylamide) (polyNIPAM) is a classic temperature-responsive polymer and has been used as the thermally responsive component in a number of systems such as simple polymer solutions, gels, microgels, films, adsorbed layers, grafted polymer layers, functionalized copolymers, micelles, and more recently block copolymers.[1−4] The appeal of polyNIPAM as a temperature-responsive polymer is that, unlike other temperature-responsive polymers such as poly(ethylene oxide), its critical temperature is nearly invariant over large concentration and molecular weight ranges,[5] making it easier to formulate. The NIPAM monomer is also polymerizable by free radical polymerization, making it accessible to modern controlled polymerization techniques, including reversible addition−fragmentation transfer (RAFT).[6−9]

RAFT and related controlled-radical techniques yield excellent control over both the molecular weight and polydispersity of the final product and dramatically simplify the preparation of block copolymers and other architectures. In many cases RAFT can afford such control over a polymerization reaction that even short homo or block co-oligomer chains can be prepared with low polydispersity. Thus, well-defined co-oligomer amphiphiles can be prepared that are more like industrial surfactant formulations, such as poly(oxyethylene) *n*-alkylethers and alkylphenols,[10,11] than block copolymers.[12−17] Such amphiphiles exhibit a rich library of self-assembly phases[18] and act as highly effective emulsifiers.[19,20]

PolyNIPAM undergoes phase separation in aqueous solution above its lower critical solution temperature (LCST) or cloud point (T_c), which lies at about 33 °C for conventional polyNIPAM in aqueous solution.[1] The LCST of NIPAM oligomers decreases slightly with increasing molecular weight.[21,22] This trend is also found for poly(ethylene oxide).[23] However, for poly(oxyethylene) alkyl ether surfactants the trend is reversed. For these the LCST increases with increasing molecular weight due to the relative influence of the hydrophobic alkyl group.[24] This effect has also been studied in polyNIPAM, where it was found that the incorporation of more hydrophobic end groups also decreases the LCST.[21] The LCST of polyNIPAM can also be decreased by copolymerization with a more hydrophobic monomer or increased by copolymerization with a less hydrophobic monomer.[25]

In oligomer molecules the RAFT agent itself can be a significant contributor to properties such as solubility and self-assembly behavior of the final product. We have, for example, used RAFT agents with dodecyl chains previously to create homo-oligomer amphiphiles with oligo(hydroxyethyl acrylate)

Received: May 14, 2014
Revised: June 18, 2014
Published: June 18, 2014

   dx.doi.org/10.1021/la501861t | *Langmuir* 2014, 30, 7986−7992

polar groups that mimic the features of the self-assembly of traditional nonionic surfactants.[18] The other singular advantage of RAFT-derived amphiphiles is that they remain active as chain-transfer agents and so can be used for the in situ polymerization of a variety of self-assembled and dispersed phases.[19,26,27]

In this work, we investigate the self-assembly of a series of temperature- and pH-responsive polyNIPAM-based surfactants as a function of molecular weight. The polyNIPAM surfactants ($C_{12}NIPAM_m$ shown in Figure 1) are prepared in a single step

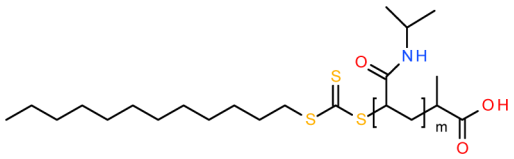

Figure 1. PolyNIPAM-based surfactants ($C_{12}NIPAM_m$).

using a RAFT agent with an *n*-dodecyl hydrophobic tail, which is long enough to induce self-assembly and typical of small-molecule surfactants. Temperature responsiveness is generated by incorporating NIPAM with a degree of polymerization in the range of values typically found in modern block co-oligomers and copolymers. pH responsiveness is added via an ionizable carboxylic acid group in the RAFT agent so that each amphiphile has exactly one ionizable group. These are similar in design to carboxylate and sulfate derivatives of poly(oxyethylene) *n*-alkyl ether surfactants widely used in personal care formulations.[28−31]

EXPERIMENTAL SECTION

NIPAM (Aldrich) was polymerized using a 4,4′-azobis(4-cyanovaleric acid) initiator (Aldrich), 2-(dodecylthiocarbonothioylthio)-2-methyl-propionic acid RAFT control agent (A. Serelis),[32] in the mole ratio *n*:0.2:1.0, where *n* is the target degree of polymerization. Samples were flushed with nitrogen for approximately 15 min and then polymerized at 70 °C in methanol (Merck) for typically 16 h to achieve greater than 95% conversion. The degrees of polymerization realized were calculated from measured molecular weights determined by size exclusion chromatography (SEC) and are given in Table 1.

Table 1. Target and Measured Degrees of Polymerization (DP_{target} and DP_{SEC}, Respectively), Number and Weight-Average Molecular Weights (M_n and M_w, Respectively), and Dispersity ($Đ$) for $C_{12}NIPAM_m$[a]

DP_{target}	DP_{SEC}	M_n	M_w	$Đ$
10	7	1110	1420	1.28
20	17	2300	2730	1.19
40	39	4720	5660	1.20
60	60	7170	8470	1.18
80	78	9210	11 060	1.20
100	96	11 200	13 400	1.19

[a]DP_{SEC}, M_n, M_w, and $Đ$ were measured using size exclusion chromatography (SEC).

Molecular weights were measured using a Polymer Laboratories PL-GPC 50 SEC with a differential refractive index detector and two PolarGel-M analytical columns (300 × 7.5 mm^2) at 50 °C. The flow rate was 0.7 mL min^{-1}, and the eluent was *N*,*N*-dimethylformamide containing 0.04 g L^{-1} hydroquinone and 0.1 wt % lithium bromide. Samples were dissolved in the eluent (with water added as a flow rate marker) and filtered prior to injection (0.45 μm PTFE filters). The molecular weights of the polymers were determined using Cirrus GPC software with a conventional calibration obtained from polystyrene standards (6.82 × 10^2 to 1.67 × 10^6 g mol^{-1}).

Surfactant penetration (flooding) scans of these polymers in contact with aqueous solutions revealed no optically birefringent phases by polarizing microscopy. Cloud points (LCSTs) were measured on an SRS OptiMelt automated melting-point apparatus at a heating rate of 4 °C min^{-1}. Cloud points were determined from an extrapolation of the measured opacity above the cloud point back to the baseline.

Small-angle neutron scattering (SANS) was measured on the Quokka SANS line[33] of the Opal reactor at the Australian Nuclear Science and Technology Organization (ANSTO) using 5 Å neutrons ($\Delta\lambda/\lambda$ = 0.065) at a single sample-to-detector distance of 3.3 m (SSD = 10 m and 30 cm detector offset) to give a q range of 0.01−0.34 $Å^{-1}$. Data reduction and analysis was performed in Igor Pro 6.31 using the NIST macros[34] modified for Quokka data sets.

SANS data was fit using the "hairy" spheroid model given by[35]

$$F_{mic}(q) = N^2B_S^2F_S(q) + NB_C^2F_C(q) + 2N^2B_SB_CS_{SC}(q) + N(N-1)B_C^2S_{CC}(q) \quad (1)$$

where $F_{mic}(q)$ is the scattering from a single micelle, $F_s(q)$ is the scattering from the spheroidal core,[36] $F_c(q)$ is the scattering from a polymer chain using the Debye equation,[37] $S_{sc}(q)$ is the scattering between the core and a polymer chain in the shell, and $S_{cc}(q)$ is the scattering between chains in the shell. N is the number of polymers per aggregate (aggregation number), $B_x = V_x\Delta\rho_x$, where V is the volume of the hydrophobic block (V_s) or polymer chain (V_c), and $\Delta\rho$ is the scattering length density difference (contrast) between the solvent (D_2O) and either the hydrophobic tail ($\Delta\rho_s$) or the polymer chain ($\Delta\rho_c$).

RESULTS AND DISCUSSION

Nonionic $C_{12}NIPAM_m$: Cloud Points. Figure 2 shows the cloud points of 1 wt % aqueous solutions of the acidic (un-

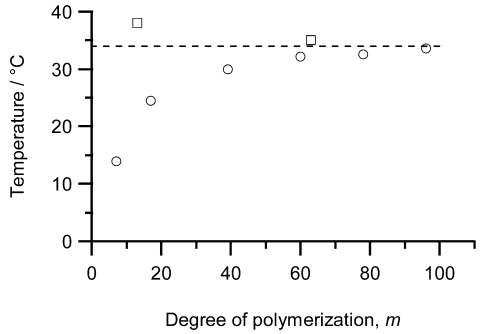

Figure 2. Cloud points (1 wt %) for $C_{12}NIPAM_m$ (in D_2O) as a function of the degree of polymerization, m. Circles are $C_{12}NIPAM_m$and squares are literature values of polyNIPAM oligomers with no hydrophobic group attached.[22]

ionized) form of $C_{12}NIPAM_m$ as a function of the degree of polymerization, m, together with literature values for polyNIPAM homo-oligomers over the same range of degree of polymerization.[22] Both samples approach the same limiting value of approximately 33 °C at high molecular weight but do so from different directions. The cloud points of the polyNIPAM oligomers decrease slightly to their final value while the $C_{12}NIPAM_7$ cloud point lies below room temperature and increases with m to the same final value. This trend for amphiphilic NIPAM appears to be due to the hydrophobicity of the tail group dominating at a low degree of polymerization to lower the LCST.[38] This is, at least qualitatively, similar to the behavior of poly(ethylene oxide)-based oligomers bearing large hydrophobic groups on one[24] or both ends.[39]

dx.doi.org/10.1021/la501861t | Langmuir 2014, 30, 7986−7992

SANS spectra for 1 wt % solutions of $C_{12}NIPAM_m$ in D_2O at 10, 20, and 30 °C are shown in Figure 3. The scattering

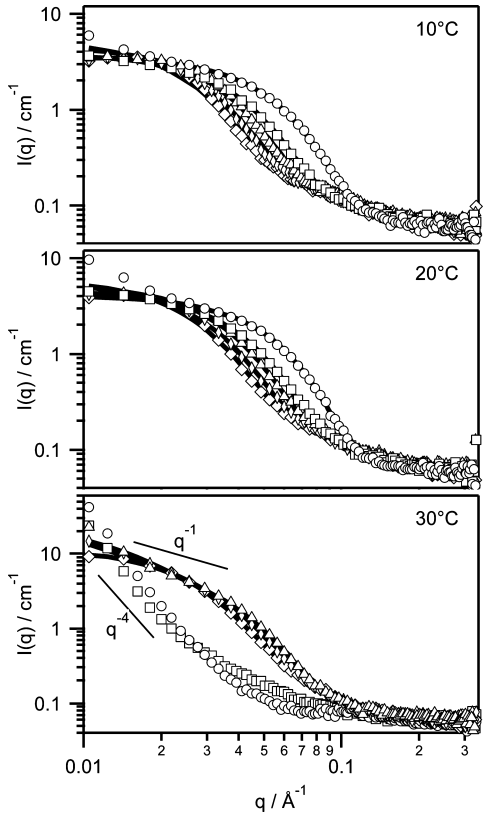

Figure 3. SANS spectra for 1 wt % $C_{12}NIPAM_m$ in D_2O at 10, 20, and 30 °C. Data is for m = 17 (○), 39 (□), 60 (Δ), 78 (◊), and 96 (◊). Solid lines are best fits to the hairy spheroid model. Fit values are in Table 2

intensity at low q is too large for individual polymer chains in solution (which would give a maximum of $I(0) \approx 0.18$ cm^{-1}, cf., $I(0) > 3$ cm^{-1} in Figure 3) and thus demonstrates the presence of small aggregates in solution. The data cannot be adequately described by simple models such as spheres, spheroids, rods, or disks nor can they be fit with core−shell versions of these models. However, excellent fits are obtained with the hairy spheroid model of Pedersen,[35] given by eq 1, which consists of a spheroidal core with semiaxes of R_a, R_a, and R_b coated with a layer of (polyNIPAM) Gaussian coils with a radius of gyration R_g. The chains decorate the core such that the center of mass is a distance R_g from the surface.

Best-fit parameters, given in Table 2, show these micelles to be nearly spherical (i.e., $R_a \approx R_b$) for all samples examined at both 10 and 20 °C. The core radii are all smaller than would be expected for a fully-extended n-dodecyl tail (~16 Å),[40] and the values systematically decrease as the NIPAM chain becomes longer. At the same time, the radius of gyration of the polyNIPAM shell increases as approximately $R_g \approx m^{0.5}$ for both the 10 and the 20 °C data (Figure 4), which is expected for a Gaussian polymer.[41] The overall micelle radius ($\sim R_a + 2R_g$) also increases with m, and this is due almost entirely to the increase in R_g. The shrinkage of the micellar core at the expense of the solvent-swollen corona is commonly seen in diblock copolymer micelles.[42] Smaller-than-expected micellar cores have also sometimes been reported in poly(oxyethylene) alkyl ether surfactants with large polar groups, but the effect is usually smaller and there are no systematic studies of this to our knowledge.[43]

At 30 °C (Figure 3(c)), $C_{12}NIPAM_{17}$ and $C_{12}NIPAM_{39}$ are both above their respective cloud points (Figure 2). SANS patterns of these samples are consistent with phase separation and the formation of large droplets, which exhibit Porod limit scattering.[44] For the longer polyNIPAM chains that remain in solution (i.e., m = 60, 78, and 96), the fit results show significant elongation of the micelles along their b axis (Table 2). Although all of the micelles are modeled as prolate spheroids for consistency, this uniaxial elongation is essentially a sphere-to rod transition, and the emergence of the expected $I(q) \approx q^{-1}$ behavior can be seen at low q in Figure 3(c) for these three non-phase-separating samples.

Accompanying the elongation of the core is a large decrease in R_g of the $NIPAM_m$ chains. As the $NIPAM_m$ corona approaches insolubility on warming and the solvent quality of the water decreases, the chains shrink toward the hydrophobic core. This reduction in R_g also affects their lateral dimensions and necessarily corresponds to a decrease in the area per headgroup for each surfactant molecule. Such a decrease in the area per polar group increases the surfactant packing parameter,[45] giving rise to the observed sphere-to-rod transition.

The R_g values of the soluble amphiphiles (Figure 4) no longer follow a power law dependence as a function of m at 30 °C, as they did at lower temperatures. Rather, the fitted R_g values are consistent with the partial collapse of the chains toward a sphere composed purely of $NIPAM_m$ (shown as a dashed line in Figure 4). This shows that the m = 60 chain, which is closest to its LCST, has almost completely collapsed but that the longer chains are still partially hydrated at 30 °C. These results are consistent with viscosity and quasi-elastic light scattering results by Kubota et al.[46] on high-molecular-weight polyNIPAM in dilute aqueous solutions, which show a chain collapse as the temperature approaches the LCST.

Ionized $C_{12}NIPAM_m$. The $C_{12}NIPAM_m$ samples were ionized by titrating the terminal carboxylic acid group with NaOH to the end point (Figure 1) to give the salt, $NaC_{12}NIPAM_m$. None of the ionized samples, from m = 7 to 96, exhibited cloud points up to the boiling point of the solvent. That is, the cloud point is completely suppressed by the addition of the single ionized group on the end of the NIPAM chain, even for the sample with the shortest NIPAM chain of m = 7. The transition from clouding to nonclouding behavior is also abrupt. In $C_{12}NIPAM_{96}$ the LCST increases only slightly up to 55% ionization and then increases rapidly to above 100 °C (Figure S1, Supporting Information), although fine control over the LCST with pH has also been shown to be possible for polyNIPAM with the right balance of pH-responsive comonomer.[38]

SANS spectra of 1 wt % solutions of ionized $NaC_{12}NIPAM_m$ in D_2O at temperatures from 10 to 50 °C are shown in Figure 5. The scattering data again demonstrates the presence of micelles in solution, with the additional feature of an interaction peak in the intermediate q range due to electrostatic repulsions between charged micelles. This data was also fit using the hairy spheroid model, this time with the addition of a structure factor to account for the screened Coulomb interactions[47,48] now present between micelles. Best-fit parameters for micelle dimensions are listed in Table 2, alongside the data for the corresponding un-ionized micelles. (See Supporting Informa-

dx.doi.org/10.1021/la501861t | Langmuir 2014, 30, 7986−7992

Table 2. Best-Fit SANS Values for Micellar Dimensions (Å) and Effective Charges in 1 wt % Solutions of $C_{12}NIPAM_m$ and $NaC_{12}NIPAM_m$ Using the Hairy Spheroid Model and Screened Coulomb Interactions[a]

		uncharged $C_{12}NIPAM_m$			charged $NaC_{12}NIPAM_m$				
temp	m	R_a	R_b	R_g	R_a	R_b	R_g	SC diam	charge
10 °C	17	14.5	15.5	12.9	12.8	12.9	12.9	64.3	15
	39	12.5	12.7	20.3	10.9	12.5	21.0	77.2	11
	60	10.8	14.4	24.8	11.3	11.7	26.9	81.8	14
	78	11.0	11.5	29.5	10.0	11.6	33.7	84.6	13
	96	9.7	12.8	33.5	9.1	14.1	39.5	85.1	13
20 °C	17	15.2	17.4	12.3	13.0	13.1	12.5	66.6	14
	39	12.8	12.9	20.0	11.7	11.9	19.4	78.8	13
	60	10.7	16.2	23.6	11.4	12.6	24.4	83.0	15
	78	10.9	13.2	27.6	10.3	12.2	30.1	87.0	13
	96	9.6	14.7	31.5	9.8	12.7	35.4	87.4	12
30 °C	17				13.7	13.8	11.6	66.5	13
	39				12.4	12.5	17.8	81.2	13
	60	18.6	304	12.5	12.0	12.1	22.4	86.5	13
	78	10.6	167	19.0	11.7	11.8	25.1	95.5	14
	96	8.8	65	22.8	11.2	12.5	28.6	101.4	14
40 °C	17				14.0	14.1	11.5	69.7	12
	39				13.5	15.0	17.0	113.4	9
	60				15.6	52.6	13.4	114.9	11
	78				16.1	60.2	16.8	128.8	13
50 °C	17				14.5	15.0	11.1	70.8	12
	39				16.5	16.8	16.2	111.0	10
	60				18.9	46.0	19.2	131.1	19
	78				28.1	64.0	24.2	152.9	22

[a]Full fit values are given in Tables S1 and S2. Errors are approximately ±0.5 Å.

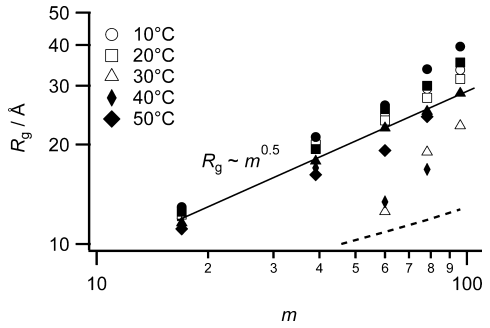

Figure 4. R_g of the NIPAM headgroup vs degree of polymerization, m, at 10 (○), 20 (□), 30 (Δ), 40 (◊), and 50 °C (◊). Open symbols are for un-ionized $C_{12}NIPAM_m$, and closed symbols are for the fully ionized form. The solid line is $R_g \approx m^{0.5}$, as expected for a Gaussian coil, and the dashed line is the R_g for an equivalent sphere of a completely collapsed polyNIPAM chain.

tion for full list of best-fit values and Figure S2 for a sample combination of form and structure factors)

Incorporating the screened Coulomb potential into the model fit yields a good description of the scattering peak position and shape but in some cases fails to describe the low-q scattering, most notably for $NaC_{12}NIPAM_{17}$. This may indicate an additional intermicellar attraction ($C_{12}NIPAM_{17}$ does have the lowest LCST in this series) or may arise from some approximations not accounted for in the models for either the form or structure factor. The Hayter–Penfold structure factor for screened Coulomb interactions calculates an equivalent or effective micelle hard sphere diameter or distance of closest approach (denoted SC diam in Table 2) and a corresponding total surface charge for each micelle. Best-fit values for both parameters are physically reasonable. The SC diameter is consistent with the charges residing in the outer part of the polyNIPAM corona, and the micelle charge is somewhat smaller than the aggregation number as estimated from the core volume ($\pi R_a^2 R_b/3$) divided by the alkyl tail volume (375 Å^3). It must be borne in mind that the micelles are not hard spheres but rather have a compressible corona and the charges are not confined to a spherical surface but may lie anywhere within the polyNIPAM corona. While this model is more than simply a useful parametrization of the peak shape, these factors caution against an overinterpretation of the quantitative SC diameter and charge values, without compromising the micelle shape information.

Charged micelles at 10 and 20 °C are, like their un-ionized counterparts, all approximately spherical with micelle core radii of $R_a \approx R_b$. In the ionized micelles this is also true at 30 °C, when the un-ionized micelles have elongated significantly or demixed. R_a again decreases as m increases. The ionized micelle cores are slightly but systematically smaller than corresponding un-ionized micelles, e.g., for $C_{12}NIPAM_{17}$ $R_a \approx R_b \approx 15$ Å (un-ionized) versus 13 Å (ionized) at 10 °C. R_g of the ionized and un-ionized micelles are indistinguishable within experimental uncertainty. This is also clear in Figure 4, which shows that the scaling of $R_g \approx m^{0.5}$ is preserved in the ionized micelles up to 30 °C. The slight change in core radii is therefore not a result of changes in the conformation of the polyNIPAM corona (as occurs on warming and desolvation of the un-ionized micelles). Rather, it is attributed to the charge on each headgroup slightly increasing repulsions with its neighbors, thus increasing the area per amphiphile. The inclusion of charge on the micelles has only a small influence on micelle structure below the LCST but does exert an influence on solution behavior through the intermicellar interactions.

dx.doi.org/10.1021/la501861t | Langmuir 2014, 30, 7986–7992

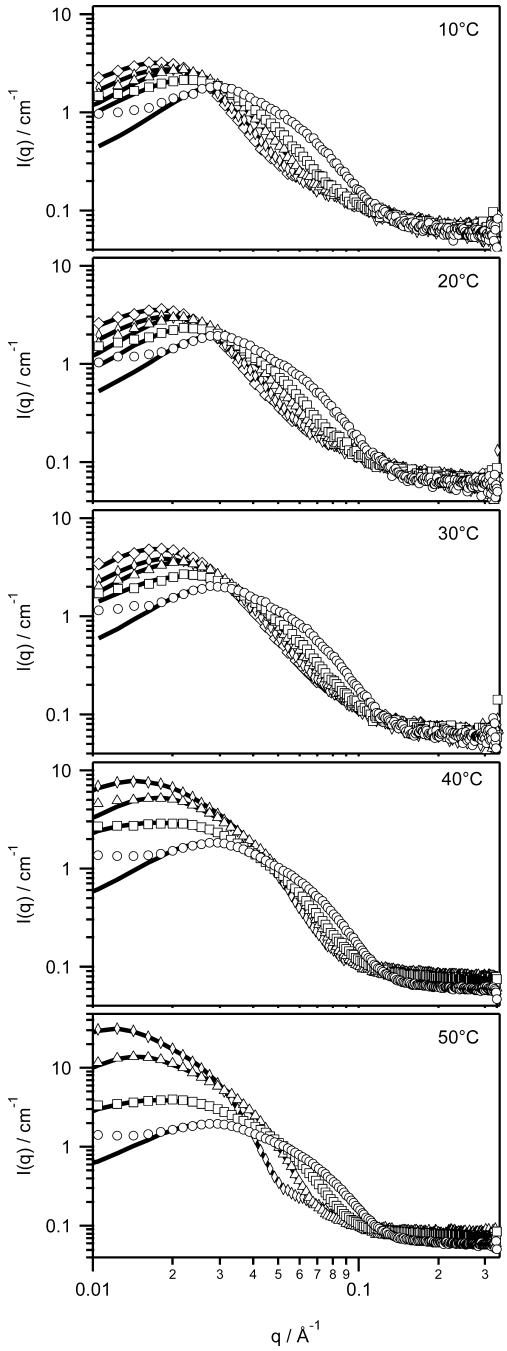

Figure 5. SANS spectra for 1 wt % fully ionized $C_{12}NIPAM_m$ in D_2O at 10, 20, 30, 40, and 50 °C. Data are for m = 17 (○), 39 (□), 60 (Δ), 78 (◊), and 96 (◊). Corresponding fits to the hairy spheroid model with screened Coulomb interactions are given in Table 2

When the temperature is increased beyond the LCST of polyNIPAM to 40 °C and then 50 °C, the behavior of the micelles depends on the length of the NIPAM chain. The conformations of shorter polyNIPAM chains (i.e., m = 17 and 39) are unaffected by the temperature increase (Figure 4), with the micelle dimensions remaining nearly unchanged at both temperatures. This is remarkable considering that the un-ionized versions of these samples completely demix from water, with the polyNIPAM chain collapsing in solution. These micelles with short polyNIPAM chains are most strongly affected by the incorporation of charge, remaining stabilized well above the expected LCST by electrostatic interactions.

Micelles with longer polyNIPAM chains ($m \geq 60$) exhibit a large increase in the scattering intensity at low q, accompanied by a shift in the scattering curve toward lower q, signaling micelle growth. The best-fit values show a small increase in the core cross-sectional radius, R_a, at 40 °C but a much more pronounced elongation via R_b. Thus, the increased scattering is caused predominantly by micelle elongation. These changes are accompanied by a decrease in R_g. Figure 4 shows that at 40 °C, R_g has decreased by an amount similar to that of the corresponding un-ionized systems at 30 °C. These longer polyNIPAM chains are less affected by a single charge and thus contract from solution toward the micelle core above the un-ionized LCST. Despite this incipient collapse, the charge on the individual amphiphiles is sufficient to stabilize these micelles electrostatically and prevent demixing from occurring in these solutions.

Further increasing the temperature to 50 °C increases both R_a and R_b. Surprisingly it is R_a that shows the larger change, and here the model reveals a dramatic change in micelle structure. Recall that the shortest radius of a micelle core cannot exceed the fully extended length of a dodecyl chain, 16.7 Å,[40] whereas the model fit yields R_a = 18.9 Å for m = 60 and 28.1 Å for m = 78 at 50 °C. This can occur only if some of the NIPAM monomers have completely collapsed out of solution to form part of the unsolvated micelle core. As the primary source of SANS contrast is hydrogen versus deuterium, the fitted core dimensions will be little affected by our failure to correct for the small difference in scattering length densities of H-alkane and H-NIPAM.

The best-fit R_g values at 50 °C do not indicate the collapse of the remaining length of the polyNIPAM corona onto the micelle core. Instead they remain extended into solution like the shorter polyNIPAM chains due to the ionic groups at their ends. This is confirmed by the fact that it was not possible to fit the scattering from any of these micelles with a core−shell model, demonstrating that the polyNIPAM chains do not completely collapse into the core. We expect that continuing to raise the temperature would increase the core radii as greater fractions of polyNIPAM collapsed out of solution. However, the absence of a cloud point in any of the ionized systems suggests that some fraction of the polyNIPAM chain near the charged center always remains hydrated and separate from the hydrophobic core. This stabilizes the micelle structure, and the intermicellar electrostatic repulsion prevents phase separation.

■ CONCLUSIONS

Using a carboxylic acid-functionalized dodecyl-chained RAFT agent, we have made a series of temperature-responsive, polyNIPAM-based surfactants with varying degrees of polymerization ($C_{12}NIPAM_m$). For the shortest NIPAM blocks, the LCST is significantly reduced due to the presence of the hydrophobic tail (e.g., for m = 7 the LCST is 13 °C). With increasing m, the LCST increases up to ∼33 °C, in agreement with unmodified polyNIPAM.

The $C_{12}NIPAM$ was shown by SANS to form micelles that can be described using a spheroidal dodecyl core coated with a hairy polymer layer. As these micelles approach their LCST and the solvent quality is reduced, the polyNIPAM chains collapse onto the hydrophobic core. This first causes an elongation of the micelles before the surfactant phase separates. Ionizing the terminal carboxylic acid group on $C_{12}NIPAM_m$ completely suppresses phase separation, leaving micelles in solution at all temperatures up to 50 °C. The temperature dependence of the

dx.doi.org/10.1021/la501861t | Langmuir 2014, 30, 7986−7992

micelle morphology is highly dependent on the degree of polymerization. The behavior of short NIPAM chains is dominated by the terminal charge and remains globular at all temperatures examined, while longer NIPAM chains collapse and micelles again elongate at higher temperatures but never macroscopically demix.

Combining pH-responsive and thermoresponsive moieties within the architecture of a surfactant with a traditional small hydrophobic tail, we have been able to separate polyNIPAM's signature temperature dependence from its solubility, allowing it to remain in solution or phase separate under different conditions. This enables independent control over micelle morphology and polar layer thickness in amphiphilically self-assembled systems. This control should easily be extended to microemulsions, vesicles, and other surfactant self-assembly phases, enabling the exploitation of control in a variety of contexts from temperature-sensitive viscoelastic solutions to the triggered release of solubilized additives.

■ ASSOCIATED CONTENT

Supporting Information

$C_{12}N_{96}$ cloud points. Full fit values for the SANS data in Figures 3 and 5 using the hairy spheroid model. Model components for interacting hairy spheroid model + screened Coulomb (HPMSA) structure factor for the fit of $C_{12}N_{80}Na$ at 30 °C. This material is available free of charge via the Internet at http://pubs.acs.org.

■ AUTHOR INFORMATION

Corresponding Author

*E-mail: gregory.warr@sydney.edu.au. Tel: +612 9351 2106.

Present Address

(S.P.) Department of Chemistry, Warwick University, Gibbet Hill, Coventry CV4 7AL, U.K., and Faculty of Pharmacy and Pharmaceutical Sciences, Monash University, VIC 3052, Australia.

Notes

The authors declare no competing financial interest.

■ ACKNOWLEDGMENTS

This work was supported by an Australian Research Council Discovery Grant. We acknowledge the support of the Bragg Institute, Australian Nuclear Science and Technology Organisation, in providing the neutron research facilities used in this work. We also thank Dr. Algi Serelis from Dulux Australia for providing the RAFT agent used in this study.

■ REFERENCES

(1) Schild, H. G. Poly(N-isopropylacrylamide): experiment, theory and application. *Prog. Polym. Sci.* **1992**, *17*, 163−249.

(2) Koga, T.; Tanaka, F.; Motokawa, R.; Koizumi, S.; Winnik, F. M. Theoretical Modeling of Associated Structures in Aqueous Solutions of Hydrophobically Modified Telechelic PNIPAM Based on a Neutron Scattering Study. *Macromolecules* **2008**, *41*, 9413−9422.

(3) Chung, J. E.; Yokoyama, M.; Suzuki, K.; Aoyagi, T.; Sakurai, Y.; Okano, T. Reversibly thermo-responsive alkyl-terminated poly(N-isopropylacrylamide) core-shell micellar structures. *Colloids Surf., B* **1997**, *9*, 37−48.

(4) Wei, H.; Cheng, S.-X.; Zhang, X.-Z.; Zhuo, R.-X. Thermo-sensitive polymeric micelles based on poly(N-isopropylacrylamide) as drug carriers. *Prog. Polym. Sci.* **2009**, *34*, 893−910.

(5) Fujishige, S.; Kubota, K.; Ando, I. Phase transition of aqueous solutions of poly(N-isopropylacrylamide) and poly(N-isopropylmethacrylamide). *J. Phys. Chem.* **1989**, *93*, 3311−3313.

(6) Chiefari, J.; Chong, Y. K.; Ercole, F.; Krstina, J.; Jeffery, J.; Le, T. P. T.; Mayadunne, R. T. A.; Meijs, G. F.; Moad, C. L.; Moad, G.; Rizzardo, E.; Thang, S. H. Living Free-Radical Polymerization by Reversible Addition−Fragmentation Chain Transfer: The RAFT Process. *Macromolecules* **1998**, *31*, 5559−5562.

(7) Moad, G.; Rizzardo, E.; Thang, S. H. Toward Living Radical Polymerization. *Acc. Chem. Res.* **2008**, *41*, 1133−1142.

(8) Perrier, S.; Takolpuckdee, P. Macromolecular design via reversible addition−fragmentation chain transfer (RAFT)/xanthates (MADIX) polymerization. *J. Polym. Sci., Part A: Polym. Chem.* **2005**, *43*, 5347−5393.

(9) Keddie, D. J.; Moad, G.; Rizzardo, E.; Thang, S. H. RAFT Agent Design and Synthesis. *Macromolecules* **2012**, *45*, 5321−5342.

(10) Nilsson, P. G.; Wennerstrom, H.; Lindman, B. Non-Ionic Micelles - Size, Shape, Hydration And Intermicellar Interactions From Self-Diffusion Studies. *Chem. Scr.* **1985**, *25*, 67−72.

(11) Rao, K. S.; Goyal, P. S.; Dasannacharya, B. A.; Kelkar, V. K.; Manohar, C.; Menon, S. V. G. Small-Angle Neutron-Scattering From Micellar Solutions of Triton X-100. *Pramana J. Phys.* **1991**, *37*, 311−319.

(12) Alexandridis, P.; Holzwarth, J. F.; Hatton, T. A. Micellization Of Poly(Ethylene Oxide)-Poly(Propylene Oxide)-Poly(Ethylene Oxide) Triblock Copolymers In Aqueous-Solutions - Thermodynamics Of Copolymer Association. *Macromolecules* **1994**, *27*, 2414−2425.

(13) Alexandridis, P.; Athanassiou, V.; Fukuda, S.; Hatton, T. A. Surface-Activity Of Poly(Ethylene Oxide)-Block-Poly(Propylene Oxide)-Block-Poly(Ethylene Oxide) Copolymers. *Langmuir* **1994**, *10*, 2604−2612.

(14) Holmqvist, P.; Alexandridis, P.; Lindman, B. Phase behavior and structure of ternary amphiphilic block copolymer-alkanol-water systems: Comparison of poly(ethylene oxide) poly(propylene oxide) to poly(ethylene oxide) poly(tetrahydrofuran) copolymers. *Langmuir* **1997**, *13*, 2471−2479.

(15) Forster, S.; Antonietti, M. Amphiphilic block copolymers in structure-controlled nanomaterial hybrids. *Adv. Mater.* **1998**, *10*, 195−217.

(16) Riess, G. Micellization of block copolymers. *Prog. Polym. Sci.* **2003**, *28*, 1107−1170.

(17) Gil, E. S.; Hudson, S. M. Stimuli-reponsive polymers and their bioconjugates. *Prog. Polym. Sci.* **2004**, *29*, 1173−1222.

(18) Heinen, J. M.; Blom, A. C. M.; Hawkett, B. S.; Warr, G. G. Phase Behavior of Amphiphilic Diblock Co-oligomers with Nonionic and Ionic Hydrophilic Groups. *J. Phys. Chem. B* **2013**, *117*, 3005−3018.

(19) Ganeva, D. E.; Sprong, E.; de Bruyn, H.; Warr, G. G.; Such, C. H.; Hawkett, B. S. Particle Formation in ab Initio RAFT Mediated Emulsion Polymerization Systems. *Macromolecules* **2007**, *40*, 6181−6189.

(20) Pham, B. T. T.; Zondanos, H.; Such, C. H.; Warr, G. G.; Hawkett, B. S. Miniemulsion Polymerization with Arrested Ostwald Ripening Stabilized by Amphiphilic RAFT Copolymers. *Macromolecules* **2010**, *43*, 7950−7957.

(21) Xia, Y.; Yin, X.; Burke, N. A. D.; Stöver, H. D. H. Thermal Response of Narrow-Disperse Poly(N-isopropylacrylamide) Prepared by Atom Transfer Radical Polymerization. *Macromolecules* **2005**, *38*, 5937−5943.

(22) Ieong, N. S.; Hasan, M.; Phillips, D. J.; Saaka, Y.; O'Reilly, R. K.; Gibson, M. I. Polymers with molecular weight dependent LCSTs are essential for cooperative behaviour. *Polym. Chem.* **2012**, *3*, 794−799.

(23) Malcolm, G. N.; Rowlinson, J. S. The thermodynamic properties of aqueous solutions of polyethylene glycol, polypropylene glycol and dioxane. *J. Chem. Soc., Faraday Trans.* **1957**, *53*, 921−931.

(24) Mitchell, D. J.; Tiddy, G. J. T.; Waring, L.; Bostock, T.; McDonald, M. P. Phase behaviour of polyoxyethylene surfactants with water. Mesophase structures and partial miscibility (cloud points). *J. Chem. Soc., Faraday Trans. 1* **1983**, *79*, 975−1000.

(25) Taylor, L. D.; Cerankowski, L. D. Preparation of films exhibiting a balanced temperature dependence to permeation by aqueous solutions—a study of lower consolute behavior. *J. Polym. Sci., Polym. Chem. Ed.* **1975**, *13*, 2551−2570.
(26) Siauw, M.; FitzGerald, P. A.; Hawkett, B. S.; Perrier, S. Thermoresponsive behavior of amphiphilic diblock co-oligomers of ethylene glycol and styrene in aqueous solution. *Soft Matter* **2013**, *9*, 7007−7015.
(27) Siauw, M.; Hawkett, B. S.; Perrier, S. Short Chain Amphiphilic Diblock Co-Oligomers via RAFT Polymerization. *J. Polym. Sci., Part A: Polym. Chem.* **2012**, *50*, 187−198.
(28) Abe, M.; Schechter, R. S.; Selliah, R. D.; Sheikh, B.; Wade, W. H. Phase Behavior Of Branched Tail Ethoxylated Carboxylate Surfactant/Electrolyte/Alkane Systems. *J. Dispersion Sci. Technol.* **1987**, *8*, 157−172.
(29) Triolo, R.; Caponetti, E.; Graziano, V. Small-angle neutron-scattering study of alkyl polyoxyethylene sulfate micelles. Effect of the number of polyoxyethylene groups on n-dodecyl polyoxyethylene sulfate in deuterium oxide/water mixtures at 25 °C. *J. Phys. Chem.* **1985**, *89*, 5743−5749.
(30) Hato, M.; Tahara, M.; Suda, Y. Colloidal properties of aqueous bivalent metal dodecylpoly(oxyethylene)sulfates and hexadecylpoly-(oxyethylene)sulfates (I). *J. Colloid Interface Sci.* **1979**, *72*, 458−464.
(31) Zoeller, N.; Blankschtein, D. Experimental Determination of Micelle Shape and Size in Aqueous Solutions of Dodecyl Ethoxy Sulfates. *Langmuir* **1998**, *14*, 7155−7165.
(32) Ferguson, C. J.; Hughes, R. J.; Nguyen, D.; Pham, B. T. T.; Gilbert, R. G.; Serelis, A. K.; Such, C. H.; Hawkett, B. S. Ab Initio Emulsion Polymerization by RAFT-Controlled Self-Assembly§. *Macromolecules* **2005**, *38*, 2191−2204.
(33) Gilbert, E. P.; Schulz, J. C.; Noakes, T. J. 'Quokka'—the small-angle neutron scattering instrument at OPAL. *Physica B* **2006**, *385*−*386*, 1180−1182.
(34) Kline, S. Reduction and analysis of SANS and USANS data using IGOR Pro. *J. Appl. Crystallogr.* **2006**, *39*, 895−900.
(35) Pedersen, J. Form factors of block copolymer micelles with spherical, ellipsoidal and cylindrical cores. *J. Appl. Crystallogr.* **2000**, *33*, 637−640.
(36) Guinier, A.; Fournet, G. *Small-Angle Scattering of X-rays*; Wiley: New York, 1955.
(37) Debye, P. Molecular-weight Determination by Light Scattering. *J. Phys. Chem.* **1947**, *51*, 18−32.
(38) Feil, H.; Bae, Y. H.; Feijen, J.; Kim, S. W. Effect of comonomer hydrophilicity and ionization on the lower critical solution temperature of N-isopropylacrylamide copolymers. *Macromolecules* **1993**, *26*, 2496−2500.
(39) Roth, P. J.; Jochum, F. D.; Forst, F. R.; Zentel, R.; Theato, P. Influence of End Groups on the Stimulus-Responsive Behavior of Poly[oligo(ethylene glycol) methacrylate] in Water. *Macromolecules* **2010**, *43*, 4638−4645.
(40) Tanford, C. *The Hydrophobic Effect: Formation of Micelles and Biological Membranes*, 2nd ed.; Wiley: New York, 1980; p 233.
(41) de Gennes, P.-G. *Scaling Concepts in Polymer Physics*; Cornell University Press: Ithaca, NY, 1979; p 324.
(42) Mortensen, K.; Brown, W. Poly(ethylene oxide)-poly(propylene oxide)-poly(ethylene oxide) triblock copolymers in aqueous solution. The influence of relative block size. *Macromolecules* **1993**, *26*, 4128−4135.
(43) FitzGerald, P. A.; Davey, T. W.; Warr, G. G. Micellar Structure in Gemini Nonionic Surfactants from Small-Angle Neutron Scattering. *Langmuir* **2005**, *21*, 7121−7128.
(44) Porod, G. Die Röntgenkleinwinkelstreuung von dichtgepackten kolloiden Systemen. *Kolloid-Z.* **1951**, *124*, 83−114.
(45) Israelachvili, J. N.; Mitchell, D. J.; Ninham, B. W. Theory of self-assembly of hydrocarbon amphiphiles into micelles and bilayers. *J. Chem. Soc., Faraday Trans. 2* **1976**, *72*, 1525−1568.
(46) Kubota, K.; Fujishige, S.; Ando, I. Solution Properties of Poly(N-isopropylacrylamide) in Water. *Polym. J.* **1990**, *22*, 15−20.
(47) Hayter, J. B.; Penfold, J. An analytic structure factor for macroion solutions. *Mol. Phys.* **1981**, *42*, 109−118.
(48) Hansen, J.-P.; Hayter, J. B. A rescaled MSA structure factor for dilute charged colloidal dispersions. *Mol. Phys.* **1982**, *46*, 651−656.